Available online at www.sciencedirect.com

ScienceDirect

IFAC PapersOnline CONFERENCE PAPER ARCHIVE

IFAC PapersOnLine 52-27 (2019) 305–310

Engineering based robot optimization methodology

Martin Švejda * **Arnold Jáger** *

* *University of West Bohemia, NTIS Research Centre, Pilsen, Czech Republic (e-mail: msvejda@ntis.zcu.cz, arnie87@ntis.zcu.cz).*

Abstract: The paper deals with the engineering based methodology for optimal design of non-standard robotic architectures. Two layer algorithm is presented for the optimization of robot kinematic parameters. The first layer includes mathematical optimization of the simplified dynamic model of the robot resulting in a priori estimation of the kinematic parameters. A general objective function for robot joint force/torque minimization is taken into account. The second layer provides an iterative approach which makes possible to adjust the kinematic parameters according to unmodeled engineering requirements. The proposed optimization approach is illustrated on the example of 5 a DoF robot for industrial degreasing machine.

Keywords: parametric optimization; robot; non-standard application

1. INTRODUCTION

The field of robotics covers wide range of robot architectures from simple robots (planar, SCARA) through mainstream of robotics (standard 6-axis industrial robot with spherical wrist) to complex robotic architectures for special application. While the common industrial robots of world-leading manufacturers (KUKA, Fanuc, ABB, etc.) have undergone a long development and their kinematic architecture as well as actuators design and control systems are well optimized, there are specific applications where their use is complicated or completely inadequate for many reasons, e.g. large footprint, robust and heavy mechanical construction, insufficient/excessive number of degrees of freedom (DoFs), protection or unsuitable mechanical arrangement. All these reasons lead to the need for research and development of new robot architectures.

Special robot architectures can achieve considerably extended functional properties when compared to conventional industrial or mobile robots. They are often employed in specific handling and pick and place applications. The other cases are devoted to the robotic structures for non-standard applications where robot kinematics have to be completely different to meet specific application requirements, e.g. inspection robots. The following examples show the special robot architectures falling in different fields of robotics. The well known Mars Rover designed by the NASA Jet Propulsion Laboratory is equipped with the 2.1 meter long robot arm [11; 23] designed for more challenging research mission. Mobile robot arm with teaching fantom device which mimics robotic arm kinematics and is used for controlling the arm is presented in [3]. The interesting field of robotics represent agriculture robots. The unmanned ground vehicle equipped with 8 DoF collaborative robot arm that permits to work in unstructured environments is shown in [15]. Efficient harvesting system [1] made by Energid company can pick a fruit every 2 to 3 seconds. The system uses flexible tubes with removal tools at one end that can be individually fired pneumatically and steered robotically, with sensor input coming from a grid of machine vision cameras. The E-series robot [17] system produced by Agrobot robotic harvesters consists of up 24 robotic arms working wirelessly as a team and it is designed for fast picking of strawberries including ripeness identification. Two tactical light resp. heavy surveillance robots (Bulldog resp. Mastiff) [18] represent the military robot. Each of them is equipped with a 4 DoF robotic arm with 2 optional axes. Medical robots are often based on special arms architectures. The best-known Da Vinci Surgical System [21] comprises three articulated arms in the first generation and four in the second generation. The Siemens ARTIS pheno [8] enables quick and precise X-ray investigations of blood vessels using a C-shaped X-ray arm which automatically moves across the patient and it is based on customization of standard serial robot architecture. Preoperative planning for the multi-arm surgical robot cooperation is presented in [31]. The kinematic control of the 6 DoF general articulated robotic arm for minimally-invasive operations is discussed in [7]. The group of the robots of non-standard kinematic architectures form the inspection robot for Non Destructive Testing (NDT) applications [10]. VENDY robot for circumferential pipe welds testing [24] or more complex robotic system SAVA [25; 30] for elbow and branch weld testing were completely designed and optimized. The latest NDT multi-redundant robot ROBIN with up to 13 DoF was introduced for inspections in very restricted areas. Virtual simulation model and control algorithm design is reported in [29; 2].

Unfortunately, introducing the non-standard and user-defined robot architectures brings the necessity of structural/parametric optimization which results in well designed, technically feasible and easy-controllable robots. Many general methods for unconstrained and constrained optimization have been presented [20; 14; 16] which can be used for robot parametric optimization problem [26]

10.1016/j.ifacol.2019.12.678

leading to dexterity optimization, joint force/velocity minimization, singularities and obstacles overcoming, etc.

2. ROBOT OPTIMAL DESIGN METHODOLOGY

On the other hand many, of optimization methods mentioned above are strictly dependent on the clear definition of the optimization problem which comprises unique objective function, constraints and robot workspace or trajectory where the robot is to be optimized. These requirements are often not fully satisfactory because of some condition arising from other restrictions which are difficult to model or can not be modeled at all, e.g. machining limitations, robot cabling and packaging, limitation resulting from mechanical design of product family (motors, gears, sensors), etc. These restrictions make impossible to use blindly the mathematical optimization background and assume we get the desired optimal robot design which is ready for manufacturing, control and use in a satisfactory manner.

Therefore, the paper presents the methodology for optimal robot kinematic design which combines the general optimization algorithms as well as iterative re-design process based on real manufacturing requirements. The proposed methodology is supported by the following steps:

Initial mathematical optimization based on the virtual simulation model: The first phase of the proposed methodology which serves for initial optimization of the kinematic parameters of the robot. The simplified virtual simulation model of the robot is derived, workspace and trajectory of the end-effector is generated and the objective function is defined. The optimal kinematic parameters of the robot are found through a chosen optimization algorithm.

Iterative parameters redesign to meet other unmodeled requirements: An iterative process where the initial robot kinematic parameters are integrated into the CAD model of the robot and the 3D Kinematic Parameters Dependent CAD (KPDCAD) model is obtained containing real links and joints dimensions, shapes, materials and actuators specification. The dynamic parameters (mass, center of gravity and inertia tensor) are obtained for each robot kinematic pairs (joints and the following arm) via appropriate decomposition of KPDCAD model (commonly available feature in CAD/CAM software). The iterative process is summarized as follows:

(1) Adjust the robot kinematic parameters according to expert's (e.g. a construction designer) requests to fulfil the real limitations.
(2) Use KPDCAD model to generate robot dynamic model.
(3) Define and evaluate the objective function (not necessarily the same as in the initial mathematical optimization).
(4) Verify the results, if expert's requests are fulfilled and objective function values are acceptable stop the iterations and continue, else go to (1).
(5) The optimal robot parameters are derived and the robot design is acceptable for the following manufacturing processes - final CAD/CAM documentation is generated.

The proposed methodology is demonstrated on the design of 5 DoF serial robot of special architecture, see Fig. 1, which is used for the spray nozzle positioning inside the cleaning chamber of the industrial degreasing machine. The design of the robot under consideration follows the previous developed serial-parallel robot AGEBOT [22; 5] (AGgressive Environment roBOT) for positioning of the technological part inside the cleaning chamber.

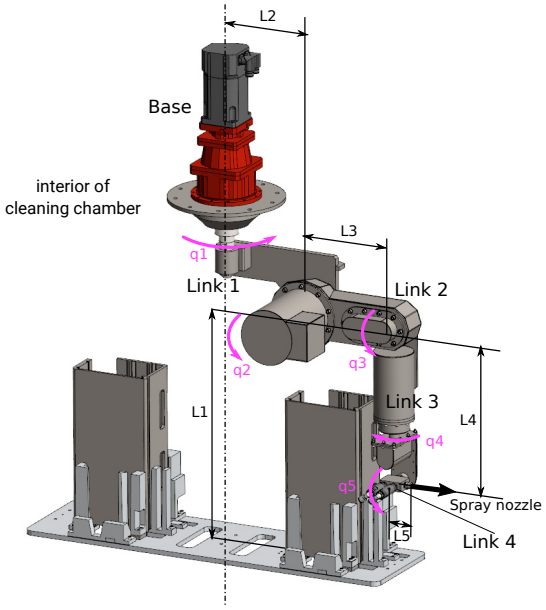

Fig. 1. Illustrative example of the robot architecture

2.1 Initial mathematical optimization

The joint resp. end-effector (spray nozzle) coordinates of the robot are defined as

$$\boldsymbol{Q} = [q_1\ q_2\ q_3\ q_4\ q_5]^T \quad \text{resp.} \quad \boldsymbol{X} = [x\ y\ z\ \alpha\ \beta]^T, \quad (1)$$

where $[x\,y\,z]$ is the position of the spray nozzle center point and α resp. β are consecutive rotations about x resp. y axis representing the spray direction $\boldsymbol{n}$

$$\boldsymbol{n} = [\sin(\beta)\ -\cos(\beta)\sin(\alpha)\ \cos(\beta)\cos(\alpha)]^T.$$

The robot kinematic parameters $\boldsymbol{\xi}$ represent the link lengths

$$\boldsymbol{\xi} = [L_1\ L_2\ L_3\ L_4\ L_5]. \quad (2)$$

The inverse kinematics for position is derived for a new introduced robot as follows:

$$q_1 = \operatorname{atan2}(Sq_1, Cq_1), \quad (3)$$

$$Sq_1 = \frac{\pm k_2\sqrt{k_1^2(k_2^2+k_1^2)}}{(k_2^2+k_1^2)k_1},\ Cq_1 = \frac{\pm\sqrt{k_1^2(k_2^2+k_1^2)}}{k_2^2+k_1^2},$$

$$[k_1\ k_2\ k_3]^T = [x\ y\ z]^T - L_5\boldsymbol{n},$$

$$q_3 = \operatorname{atan2}(Sq_3, Cq_3), \quad (4)$$

$$Sq_3 = \frac{l_1^2+l_2^2-L_3^2-L_4^2}{2L_3L_4},\ Cq_3 = \pm\sqrt{1-Sq_3^2},$$

$$\begin{bmatrix} l_1 \\ l_2 \\ l_3 \end{bmatrix} = \begin{bmatrix} Sq_1k_2 - L_2 + k_1Cq_1 \\ k_3 - L_1 \\ Sq_1k_1 - Cq_1k_2 \end{bmatrix},$$

$$q_2 = \operatorname{atan2}\left(Sq_2, Cq_2\right), \tag{5}$$
$$Sq_2 = \frac{L_4 Sq_3 l_2 + L_3 l_2 + l_1 L_4 Cq_3}{L_4^2 + 2L_4 L_3 Sq_3 + L_3^2},$$
$$Cq_2 = \frac{-l_2 L_4 Cq_3 + l_1 L_4 Sq_3 + l_1 L_3}{L_4^2 + 2L_4 L_3 Sq_3 + L_3^2},$$

$$q_5 = \operatorname{atan2}\left(Sq_5, Cq_5\right), \tag{6}$$
$$Sq_5 = -m_3,\ Cq_5 = \pm\sqrt{m_1^2 + m_2^2},$$

$$\begin{bmatrix} m_1 \\ m_2 \\ m_3 \end{bmatrix} = \begin{bmatrix} Cq_1 Cq_{23} & Sq_1 Cq_{23} & Sq_{23} \\ Sq_1 & -Cq_1 & 0 \\ Cq_1 Sq_{23} & Sq_1 Sq_{23} & -Cq_{23} \end{bmatrix} \boldsymbol{n}, \tag{7}$$
$$Sq_{23} = \sin(q_2 + q_3),\ Cq_{23} = \cos(q_2 + q_3),$$

$$q_4 = \operatorname{atan2}\left(Sq_4, Cq_4\right), \tag{8}$$
$$Sq_4 = \frac{m_2}{Cq_5},\ Cq_4 = \frac{m_1}{Cq_5}.$$

The forward kinematics for position as well as velocity and acceleration dependency between joint and end-effector coordinates and dynamic model can be computed generally for serial robots [19] through Denavit-Hartenberg notation [4]. The dynamic model of the robot is

$$\boldsymbol{M}(\boldsymbol{Q})\ddot{\boldsymbol{Q}} + \boldsymbol{C}(\boldsymbol{Q}, \dot{\boldsymbol{Q}})\dot{\boldsymbol{Q}} + \boldsymbol{G}(\boldsymbol{Q}) = \boldsymbol{\tau}\boldsymbol{F} \tag{9}$$

where $\boldsymbol{M}, \boldsymbol{C}, \boldsymbol{G}$ are appropriate dynamic matrices/vectors, $\boldsymbol{\tau}$ resp. $\boldsymbol{F}$ are joint resp. end-effector external forces/torques and $\boldsymbol{J}(\boldsymbol{Q})$ is the kinematic Jacobian which maps the joint velocity to translation resp. angular velocity of the end-effector coordinate system. The simplified "rod" model of

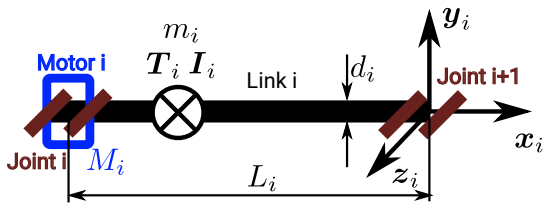

Fig. 2. Simplified robot link

the robot link is shown in Fig. 2 and the dynamic parameters of i-th link dependent on the kinematic parameters (link length) are expressed:

$$m_i = 1/4\,\pi\, {d_i}^2 \rho\, L_i + M_i,\ \boldsymbol{T}_i = \left[-\frac{\pi\, {d_i}^2 \rho\, {L_i}^2}{2\,\pi\, {d_i}^2 \rho\, L_i + 8\, M_i}\ 0\ 0 \right]^T,$$
$$\boldsymbol{I}_i = \begin{bmatrix} 1/32\,\pi\, {d_i}^4 \rho\, L_i \\ 4\,\frac{\rho\left({L_i}^3 {d_i}^2 \pi\,\rho + 3/4\,\pi\, {d_i}^4 \rho\, L_i + 16\, M_i {L_i}^2 + 3\, M_i {d_i}^2\right) {d_i}^2 L_i \pi}{192\,\pi\, {d_i}^2 \rho\, L_i + 768\, M_i} \\ 4\,\frac{\rho\left({L_i}^3 {d_i}^2 \pi\,\rho + 3/4\,\pi\, {d_i}^4 \rho\, L_i + 16\, M_i {L_i}^2 + 3\, M_i {d_i}^2\right) {d_i}^2 L_i \pi}{192\,\pi\, {d_i}^2 \rho\, L_i + 768\, M_i} \end{bmatrix}, \tag{10}$$

where m_i is a mass, $\boldsymbol{T}_i$ is a center of gravity, $\boldsymbol{I}_i$ is an inertia tensor of the ith-link of length L_i, diameter d_i and density ρ. The motor is modeled as an added mass M_i at the beginning of the link.

The optimization criterion is based on a measure published in [27]. Let's assume that the robot is supposed to move from the steady state ($\dot{\boldsymbol{X}} = \boldsymbol{0} \Rightarrow \dot{\boldsymbol{Q}} = \boldsymbol{0}$) in any direction in the required workspace with a maximum required acceleration, see Fig. 3,

$$\max_{\boldsymbol{X} \in \boldsymbol{X}_{\mathbf{opt}}} \|\ddot{\boldsymbol{X}}\| = a_{\max}.$$

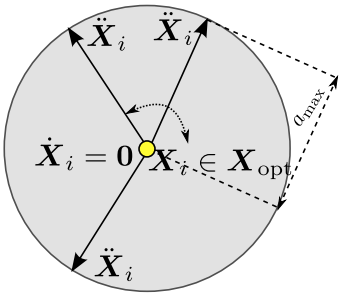

Fig. 3. Robot workspace with the end-effector acceleration definition

It was proven that the maximum 2-norm joint forces/torques for the end-effector to be at the position $\boldsymbol{X}$ (corresponding joint position $\boldsymbol{Q}$) and moving from the steady state in any direction with maximum acceleration $a_{\max}$ is given as:

$$\|\boldsymbol{\tau}\| \le \sigma_{max}\left(\boldsymbol{M}(\boldsymbol{Q}) \cdot \boldsymbol{J}^{-1}(\boldsymbol{Q})\right) \cdot \|\ddot{\boldsymbol{X}}\| + \|\boldsymbol{G}(\boldsymbol{Q})\|,$$
$$\|\boldsymbol{\tau}\|_{\max} = \sigma_{max}\left(\boldsymbol{M}(\boldsymbol{Q}) \cdot \boldsymbol{J}^{-1}(\boldsymbol{Q})\right) \cdot a_{max} + \|\boldsymbol{G}(\boldsymbol{Q})\|, \tag{11}$$

where $\sigma_{\max}(\star)$ is the maximal singular value of the matrix.

Note, that the constant $a_{\max}$ represents a weighting factor between the static optimization ($a_{\max} = 0$) and dynamic optimization ($a_{\max} >> 0$, the influence of the gravity is almost neglected, e.g. in high speed applications).

The initial optimization is defined as follows:

$$\boldsymbol{\xi}^{\star} = \underset{\boldsymbol{\xi}}{\operatorname{argmax}} \left(\min_{\boldsymbol{X} \in \boldsymbol{X}_{\mathrm{opt}}} J(\boldsymbol{X}, \boldsymbol{\xi}) \right), \tag{12}$$

$$J(\boldsymbol{X}, \boldsymbol{\xi}) = \frac{1}{J_{\mathrm{pen}} + \|\boldsymbol{\tau}\|_{\max}}, \tag{13}$$

where J is an objective function, $\boldsymbol{X}$ is the position of the end-effector from a required robot workspace $\boldsymbol{X}_{\mathrm{opt}}$ and J_{pen} is so-called penalty function which makes possible to integrate equality/inequality constraints in a simple and effective way [20] and transform the constrained optimization problem to an unconstrained one. The penalty function is assumed to limit the range of the optimized robot kinematic parameters.

The optimization problem (12) was solved in Matlab through simplex search method `fminsearch` [12].

Resolving the optimization problem (12), we get the optimal robot kinematic parameters $\boldsymbol{\xi}^{\star}$ which ensure that the 2-norm joint forces/torques of the robot over the workspace which have to be applied to reach the maximum end-effector acceleration $a_{\max}$ in any direction (from steady-state) will be minimized. Therefore, the initial robot kinematic parameters estimation supported by the mathematical background is found.

2.2 Iterative parameters redesign

The CAD model of the robot including the desired end-effector trajectory as an restriction of the robot workspace is depicted in Fig. 4. The trajectory was designed in SolidWorks as a point cloud and exported to Excel sheet. The coincidence points were interpolated by the line segments with polynomial blending (Matlab), see Fig. 5, and the feedrate for demanded velocity profile (bang-bang accelera-

tion profile with max. velocity $V_{\max}$ and max. acceleration $A_{\max}$, see Fig. 6) along the trajectory was computed with regards to velocity limitation of the robot joints (feedrate correction), for more details see [28].

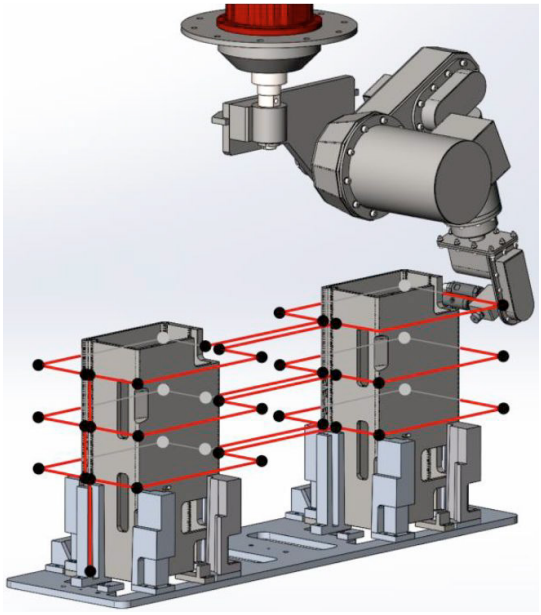

Fig. 4. CAD model of the robot and exported coincidence points

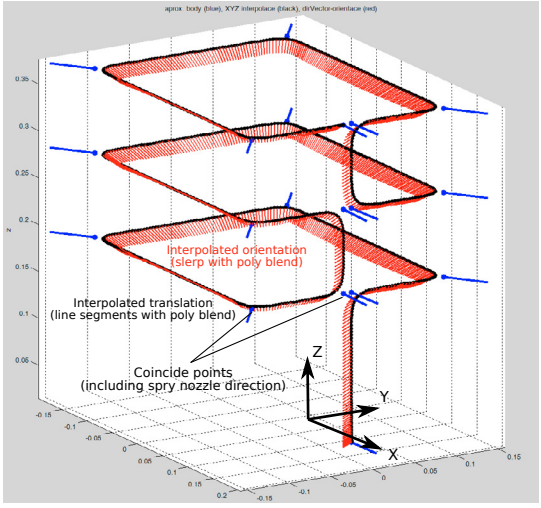

Fig. 5. Coincidence points interpolation

The KPDCAD model respecting the real structural design of the robot joints and links was decomposed, see Fig. 7, and the real dynamic parameters (generally different from the simplified "rod" dynamic model (10) mentioned above) were exported (CAD software routine). The resulting dynamic model of the robot was used for the following verification dependent on the new objective function which took into account the engineering requirements.

The *takt time* T_{end} was chosen as an independent variable and the joint velocity, acceleration and torque represented the outputs of the new objective function. Therefore the velocity profile with respect to max. acceleration $A_{\max}$ and takt time T_{end} results in a new velocity, see Fig. 6:

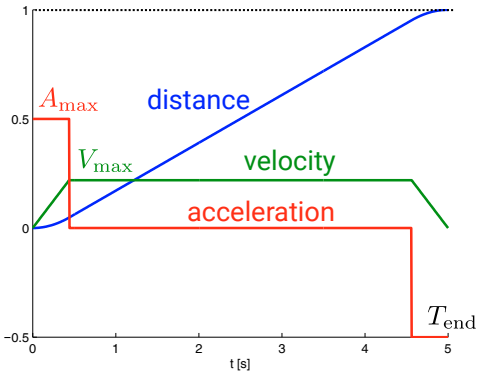

Fig. 6. Trajectory feed profile

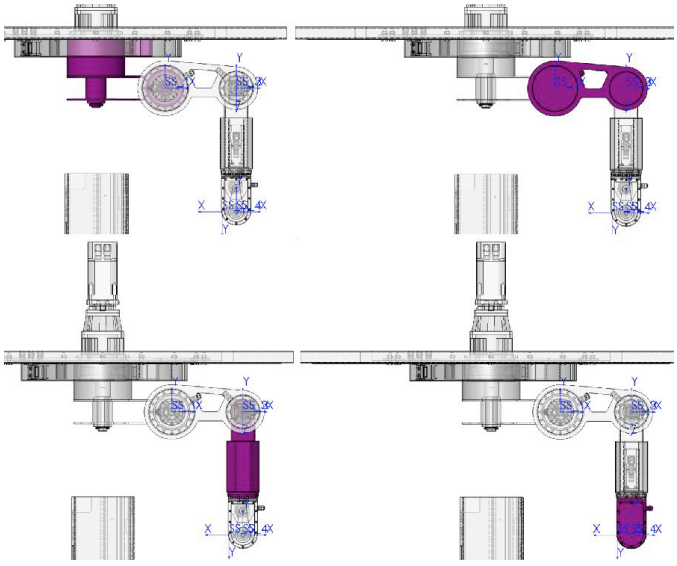

Fig. 7. CAD model decomposition

$$\bar{V}_{\max} = \frac{1}{2} A_{\max} \left(T_{\text{end}} - \sqrt{T_{\text{end}}^2 - \frac{4}{A_{\max}}} \right). \qquad (14)$$

Inverse kinematics and inverse dynamic model were used for evaluating joint velocity, acceleration and torque for the planed end-effector trajectory parametrized by the takt time.

3. RESULTS AND CONCLUSION

The initial robot kinematic parameters obtained from the mathematical optimization:

$$\boldsymbol{\xi}^{\star} = [0.55\ 0.232\ 0.389\ 0.283\ 0.1]\ [m]. \qquad (15)$$

The following CAD modelling of the robot and the iterative process of adjusting the kinematic parameters to fulfil the engineering requirements (especially cabling and links collision limitation) result in the final robot kinematic parameters:

$$\boldsymbol{\xi}^{\star} = [0.7\ 0.232\ 0.239\ 0.4136\ 0.471]\ [m]. \qquad (16)$$

The Fig. 8 illustrates the resulting takt time T_{end} depending on the required one. The reduction can be shown at the beginning of the graph where the max. robot joint velocity limitation (feedrate correction) leads to slowing

down of the end-efector along the planned trajectory. The Fig. 9 shows the maximum joint velocity, acceleration and torque depending on the resulting takt time. This dynamical study allows to verify the correct dimensioning of the robot actuators with respect to the minimum takt time.

The proposed methodology for engineering optimization was used for rapid prototyping of several other robots of non-standard architectures which have been developed at the NTIS research centre for key industrial partners. Despite the fact that the methodology does not provide generic fully automated tool for robot optimization, its main advantages can be summarized as follows:

- A priori robot parameters estimation is supported by the model based design approach (simplified dynamic model, general objective function).
- Unmodeled engineering requirements are taken into account based on iterative parameters adjustment supported by the robot CAD model.

Moreover the following control system design tasks which have to be taken into account for non-standard robot architectures are also addressed to NTIS research centre and some of them can be found in [9; 6; 13].

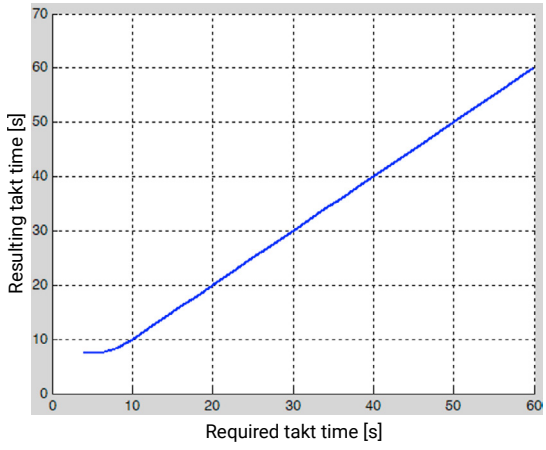

Fig. 8. Resulting robot takt time

ACKNOWLEDGEMENTS

This work was supported by the project InteCom No. CZ.02.1.01/0.0/0.0/17_048/0007267 of the Czech Ministry of Education, Youth and Sports and the Technology Agency of the Czech Republic under Competence Centre CIDAM (Center for Intelligent Drives and Advanced Machine Control) No. TE02000103.

REFERENCES

[1] C. Aloisio, R. K. Mishra, C. Chang, and J. English. Next generation image guided citrus fruit picker. In *2012 IEEE International Conference on Technologies for Practical Robot Applications (TePRA)*, pages 37–41, April 2012. doi: 10.1109/TePRA.2012.6215651.

[2] L. Bláha and M. Švejda. Path planning of hyper-redundant manipulator in developed view. In *2018 19th International Carpathian Control Conference (ICCC)*, pages 295–300, May 2018. doi: 10.1109/CarpathianCC.2018.8399644.

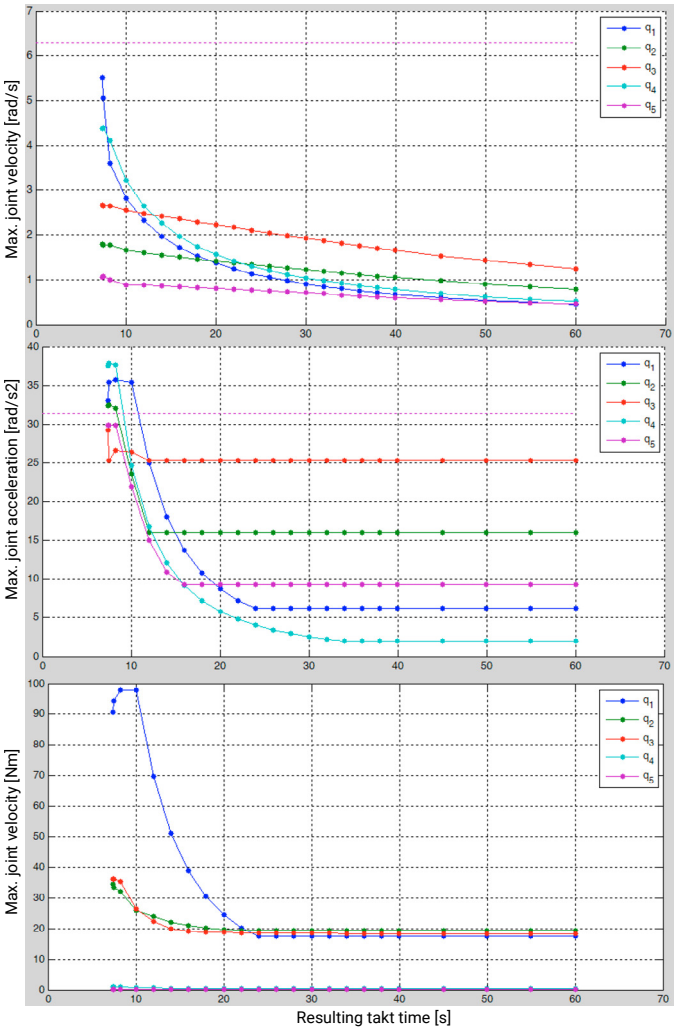

Fig. 9. Maximum joint velocity, acceleration and torque

[3] P. Czaplicki, M. Rećko, and J. Tołstoj-Sienkiewicz. Robotic arm control system for mars rover analogue. In *2016 21st International Conference on Methods and Models in Automation and Robotics (MMAR)*, pages 1122–1126, Aug 2016. doi: 10.1109/MMAR.2016.7575295.

[4] J. Denavit and R. S. Hartenberg. A kinematic notation for lower-pair mechanisms based on matrices. *Trans. of the ASME. Journal of Applied Mechanics*, 22:215–221, 1955. URL `http://ci.nii.ac.jp/naid/10008019314/en/`.

[5] M. Goubej and M. Švejda. Dynamic analysis and control of robotic manipulator for chemically aggressive environments. In *2013 IEEE International Conference on Mechatronics (ICM)*, pages 273–278, Feb 2013. doi: 10.1109/ICMECH.2013.6518548.

[6] M. Goubej, T. Popule, and A. Krejčí. Friction compensation in mechatronic systems. In *2017 18th International Carpathian Control Conference (ICCC)*, pages 93–98, May 2017. doi: 10.1109/CarpathianCC.2017.7970377.

[7] S. Gupta, S. T. Sarkar, and A. Kumar. Kinematic control of an articulated minimally invasive surgical robotic arm. In *2016 IEEE 1st International Conference on Power Electronics, Intelligent Control and Energy Systems (ICPEICES)*, pages 1–5, July 2016.

doi: 10.1109/ICPEICES.2016.7853054.

[8] Siemens Healthineers. Artis pheno – cutting-edge robotic imaging for multidisciplinary utilization. online, 2019. URL https://www.siemens-healthineers.com/clinical-specialities/surgery/surgery-product-portfolio/hybrid-or.

[9] V. Helma, M. Goubej, and O. Ježek. Acceleration feedback in PID controlled elastic drive systems. *IFAC-PapersOnLine*, 51(4):214 – 219, 2018. ISSN 2405-8963. doi: https://doi.org/10.1016/j.ifacol.2018.06.068. URL http://www.sciencedirect.com/science/article/pii/S2405896318303641. 3rd IFAC Conference on Advances in Proportional-Integral-Derivative Control PID 2018.

[10] A. Jáger, T. Čechura, and M. Švejda. Non-standard robots for NDT of pipe welds. In *2018 19th International Carpathian Control Conference (ICCC)*, pages 196–200, May 2018. doi: 10.1109/CarpathianCC.2018.8399627.

[11] Calif. Jet Propulsion Laboratory, Pasadena. Robotic arm for the mars 2020 rover. online, 2019. URL https://mars.nasa.gov/mars2020/.

[12] J. C. Lagarias, J. A. Reeds, M. H. Wright, and P. E. Wright. Convergence properties of the Nelder-Mead simplex method in low dimensions. *SIAM Journal of Optimization*, 9:112–147, 1998.

[13] N. Nevaranta, M. Goubej, T. Lindh, M. Niemelä, and O. Pyrhönen. Non-parametric frequency response estimation of two-mass-system using Kalman filter. In *2016 18th European Conference on Power Electronics and Applications (EPE'16 ECCE Europe)*, pages 1–9, Sep. 2016. doi: 10.1109/EPE.2016.7695535.

[14] J. Nocedal and S. J. Wright. *Numerical Optimization*. Springer New York, 2006. ISBN 978-0-387-40065-5.

[15] G. Quaglia, C. Visconte, L. S. Scimmi, M. Melchiorre, P. Cavallone, and S. Pastorelli. Robot arm and control architecture integration on a UGV for precision agriculture. In Tadeusz Uhl, editor, *Advances in Mechanism and Machine Science*, pages 2339–2348, Cham, 2019. Springer International Publishing. ISBN 978-3-030-20131-9.

[16] G.V. Reklaitis, A. Ravindran, and K.M. Ragsdell. *Engineering Optimization: Methods and Applications*. A Wiley-Interscience Publication. Wiley, 1983. ISBN 9780471055792. URL https://books.google.cz/books?id=Tj6NJGvk7b4C.

[17] AGROBOT robotic harvesters. Agrobot E-series. online, 2019. URL http://agrobot.com/.

[18] SDR Tactical Robots. LT2/F "Bulldog" and HD2 "Mastiff" - light tracked and heavy duty robot with arm. online, 2019. URL http://sdrtactical.com/.

[19] L. Sciavicco and B. Siciliano. *Modelling and Control of Robot Manipulators*. Advanced Textbooks in Control and Signal Processing. Springer London, 2000. ISBN 9781852332211. URL http://books.google.fr/books?id=v9PLbcYd9aUC.

[20] J. Snyman. *Practical Mathematical Optimization: An Introduction to Basic Optimization Theory and Classical and New Gradient-Based Algorithms*. Applied Optimization. Springer, 2005. ISBN 9780387243481. URL http://books.google.cz/books?id=0tFmf_UKl7oC.

[21] L. Sun, F. Van Meer, Y. Bailly, and C. K. Yeung. Design and development of a Da Vinci surgical system simulator. In *2007 International Conference on Mechatronics and Automation*, pages 1050–1055, Aug 2007. doi: 10.1109/ICMA.2007.4303693.

[22] M. Švejda and M. Goubej. Innovative design and control of robotic manipulator for chemically aggressive environments. In *Proceedings of the 13th International Carpathian Control Conference (ICCC)*, pages 715–720, May 2012. doi: 10.1109/CarpathianCC.2012.6228739.

[23] E. Tunstel, M. Maimone, A. Trebi-Ollennu, J. Yen, R. Petras, and R. Willson. Mars exploration rover mobility and robotic arm operational performance. In *2005 IEEE International Conference on Systems, Man and Cybernetics*, volume 2, pages 1807–1814 Vol. 2, Oct 2005. doi: 10.1109/ICSMC.2005.1571410.

[24] T. Čechura, A. Jáger, and M. Švejda. *User guide: Manipulator for inspection of pipes, especially for inspection pipe welds with restricted access (in Czech)*, 2016.

[25] M. Švejda. New robotic architecture for NDT applications. *IFAC Proceedings Volumes*, 47(3):11761 – 11766, 2014. ISSN 1474-6670. doi: https://doi.org/10.3182/20140824-6-ZA-1003.00989. URL http://www.sciencedirect.com/science/article/pii/S1474667016434877. 19th IFAC World Congress.

[26] M. Švejda. *Optimization of robot architectures (in Czech)*. PhD thesis, Západočeská univerzita v Plzni, 2016. URL http://home.zcu.cz/~msvejda/_publications/2016/4_SvejdaMartin_thesis_2016_06_14.pdf.

[27] M. Švejda. New kinetostatic criterion for robot parametric optimization. In *2017 IEEE 4th International Conference on Soft Computing Machine Intelligence (ISCMI)*, pages 66–70, Nov 2017. doi: 10.1109/ISCMI.2017.8279599.

[28] M. Švejda. Dynamic analysis of the manipulator for industrial cleaning chamber (DV075) (in Czech). Technical report, University of West Bohemia, 2017. URL http://home.zcu.cz/~msvejda/_publications/2017/7_dynAnalyza.pdf.

[29] M. Švejda. Virtual simulation models for ADRA-2I NDT robot. Technical report, University of West Bohemia, 2018. URL http://home.zcu.cz/~msvejda/_publications/2018/02_ROBIN_virtSimModel.pdf.

[30] M. Švejda and T. Čechura. Interpolation method for robot trajectory planning. In *2015 20th International Conference on Process Control (PC)*, pages 406–411, June 2015. doi: 10.1109/PC.2015.7169997.

[31] F. Zhang, Z. Yan, and Z. Du. Preoperative planning for the multi-arm surgical robot using PSO-GP-based performance optimization. In *2017 IEEE International Conference on Robotics and Automation (ICRA)*, pages 4208–4214, May 2017. doi: 10.1109/ICRA.2017.7989484.